Winter Precipitation Type from Microwave Radiometers in New York State Mesonet Profiler Network

BHUPAL SHRESTHA,[a] J. WANG,[a] J. A. BROTZGE,[b] AND NATHAN BAIN[a]

[a] *New York State Mesonet, University at Albany, State University of New York, Albany, New York*
[b] *Kentucky Climate Center, Department of Earth, Environmental, and Atmospheric Sciences, Western Kentucky University, Bowling Green, Kentucky*

(Manuscript received 28 February 2023, in final form 10 May 2023, accepted 22 June 2023)

ABSTRACT: Winter precipitation is a major cause of vehicle accidents, aviation delays, school and business closures, injuries through slips and falls, and adverse health impacts such as cardiac arrests and deaths. However, an improved ability to monitor and predict winter precipitation type (p-type) could significantly reduce and mitigate these adverse impacts. This study presents and evaluates a modified parcel thickness method to derive p-type from a microwave radiometer (MWR) every 10 min. The MWR-retrieved p-types from six selected New York State Mesonet (NYSM) profiler network sites are validated against reference observations from the Meteorological Phenomena Idenfication Near the Ground (mPING) and Automated Surface Observing System (ASOS). Between the two reference observations, the mPING reports are biased toward snow (SN) and sleet (SLT) and away from rain (RA) and freezing rain (FZR) compared to the ASOS. The MWR has the best Pierce skill score (PSS) for RA, followed by SN, FZR, and SLT, and consistently overforecasts FZR and underforecasts SLT compared to both mPING and ASOS. The MWR p-type retrievals are generally found to be in better agreement with ASOS than mPING. Continuous thermodynamic profiles and p-type estimates from across all 17 profiler sites are available at http://www.nysmesonet.org/networks/profiler. Having such thermodynamic information from across the state can be a valuable resource, with a significant advantage over twice daily NWS radiosondes, for monitoring and tracking hazardous winter weather in real time, for accurate forecasting, and for issuing timely warnings and alerts.

SIGNIFICANCE STATEMENT: Accurate prediction and monitoring of winter precipitation type (p-type) is important due to the adverse economic and health impacts posed by winter weather. However, complexities in understanding and modeling the processes that govern p-type and inadequate observational data limit accurate monitoring and prediction. To address these issues, a ground-based microwave radiometer (MWR) that provides thermodynamic profiles up to 10 km every 2 min, as deployed at 17 sites in the New York State Mesonet (NYSM) profiler network, can be a valuable tool. This study evaluates the accuracy of p-type estimates based on the parcel thickness method from the MWR data and its implementation to the NYSM real-time operations.

KEYWORDS: Mixed precipitation; Algorithms; Microwave observations; Atmospheric profilers; Nowcasting

1. Introduction

Hazardous winter weather conditions posed by freezing rain, snow, and sleet (ice pellet) present adverse impacts to schools and businesses, transportation, aviation, utilities, and communications that directly affect people's daily lives. According to the USDOT Federal Highway Administration (2014), over 1300 people are killed and more than 116 000 people are injured in vehicle accidents annually in the United States due to hazardous winter precipitation. The NOAA/National Centers for Environmental Information estimates that the winter weather causes approximately $2 billion (U.S. dollars) in damages annually (NCEI 2022). In addition, the hazardous winter weather events also lead to injuries by slips, trips, and falls and affect human health by increasing risk of acute myocardial infarction and cardiac arrest and sometimes leading to cardiac death (Bhaskaran et al. 2009; Dahlquist et al. 2016; Ryti et al. 2017). Therefore, more accurate monitoring and forecasting of winter precipitation types (rain, snow, freezing rain, and sleet/ice pellets) could help mitigate at least some of these impacts.

Accurate forecasting and monitoring of precipitation type (p-type) has been a long ongoing challenge (Ralph et al. 2005), but with limited success (Elmore et al. 2015). Operational forecasting models such as the North American Mesoscale Forecast System (NAM), Rapid Refresh (RAP), High-Resolution Rapid Refresh (HRRR) and Global Forecast System (GFS) are found reliable in forecasting snow and rain but have high uncertainties in forecasting freezing rain and sleet (Reeves et al. 2014; Elmore et al. 2015). Model uncertainty could be due to 1) insufficient understanding of microphysical processes that determine surface p-type (Elmore et al. 2015), and 2) lack of observational data with high spatiotemporal resolution with which to train numerical models. It is well known that the vertical profiles of temperature and moisture above-ground determine the p-type observed at the surface (Bourgouin 2000; Ahrens and Henson 2018), but these profile data are not routinely measured, despite their immense need. Though such data are readily available from the National Weather Service (NWS) radiosonde network (https://www.weather.gov/upperair/nws_upper), they are only available

Corresponding author: Bhupal Shrestha, bshrestha@albany.edu

DOI: 10.1175/WAF-D-23-0035.1

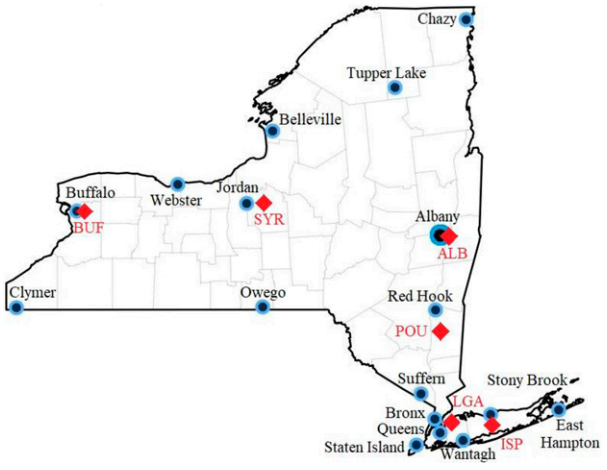

FIG. 1. A map of New York State Mesonet profiler network (black dots with blue outlines) along with six selected ASOS sites (red diamonds).

twice daily (0000 and 1200 UTC) and have low spatial coverage (only three in New York State), and are insufficient to understand highly variable microphysical processes and the resulting atmospheric state that governs p-type. And while the p-type algorithms have been developed extensively based on radiosonde profiles (Bourgouin 2000; Reeves et al. 2014; Reeves 2016), the twice daily radiosonde data are not frequent enough to adequately retrieve and monitor rapidly evolving changes in p-type. Overall, the low temporal sampling and sparse spatial coverage of radiosondes limit our ability to monitor the fine-scale microphysical and thermodynamic processes that govern p-type, particularly freezing rain and sleet because of their high variability in space and time (Elmore et al. 2015).

Recent advances in remote sensing profiling technologies now provide a plethora of opportunities for monitoring the atmosphere at high vertical and temporal resolutions. One such sensor is the ground-based microwave radiometer (MWR) that measures vertical profiles of thermodynamic variables autonomously and continuously. The MWR is a significant advantage over radiosondes as it provides a more cost-effective means for real-time monitoring of vertical profiles of temperature and moisture up to 10 km AGL every ~2 min. Furthermore, a dense network of MWRs can fill the spatial gaps of the NWS radiosonde network. To demonstrate the value of a network of profiling instruments, the New York State Mesonet (NYSM) developed a profiler network (Shrestha et al. 2021; www.nysmesonet.org/networks/profiler) comprised of 17 stations deployed across New York State (NYS, Fig. 1). Each site consists of a collocated Vaisala/Leosphere 100S scanning Doppler lidar and a Radiometrics MP-3000A microwave radiometer. The NYSM profiler network has been fully operational since 2018, and the data are distributed to researchers and forecasters from across the state and agencies like NWS and NASA.

The Radiometrics MWR measures downwelling brightness temperatures in the water vapor and oxygen bands, the 21 K-band (22–30 GHz) and 14 V-band (51–59 GHz) channels, that then are converted into profiles of temperature, liquid density, vapor density, and relative humidity. The conversion process uses a radiative transfer model trained by a neural network; the neural network is derived from multiyear radiosonde data from site(s) with similar climatology to the MWR location (Ware et al. 2003). The MWR provides vertical profiles from the surface to 10 km with a vertical resolution of 50–250 m every ~2 min. Given that the MWR retrieval is an ill-posed problem due to poor neural network performance, calibration and model uncertainties, the accuracies of the MWR-retrieved temperature and water vapor density are highest near the surface and degrade along the height (Shrestha et al. 2022; Illingworth et al. 2019; Xu et al. 2015; Cimini et al. 2015; Löhnert and Maier 2012). The study by Shrestha et al. (2022) shows that the cold biases are observed throughout the MWR-retrieved temperature profiles and can be as high as 6°C whereas dry biases are observed in water vapor density profiles within the boundary layer (~2 km) and can be as high as 1 g m^{-3} (Note: recent changes to the MWR calibration technique by Radiometrics to replace biannual liquid nitrogen calibration have significantly improved cold biases in MWR temperature profiles). Moreover, the accuracy of the MWR retrievals is also affected by the precipitation. The thin layer of water and ice accumulating on top of the MWR antenna radome affects the incoming microwave energy passing through the radome leading to high brightness temperature measurements. Therefore, it is recommended that the off-zenith measurements (20° elevation) are used during precipitation days, that have minimal impact from the precipitation and provide higher accuracy than zenith measurements (Xu et al. 2014). In general, though the MWR lacks high resolution vertical details along the profile due to its coarser resolution, the MWR observations are found to be robust for retrieving column integrated variables and parcel thicknesses (Shrestha et al. 2022). Therefore, given the higher temporal resolution of the MWR data (every ~2 min), the MWR presents a significant advantage for continuous monitoring of thermodynamic changes, and yet a relatively little attention has been given to extending the application of the MWR to retrieve and monitor winter p-type. Fortunately, several p-type algorithms have been developed based on the radiosonde profiles (Derouin 1973; Cantin and Bachand 1993; Ramer 1993; Baldwin et al. 1994; Bourgouin 2000; Schuur et al. 2012), and these can be easily applied to the MWR-retrieved profiles.

The main goal of the study is to refine the existing p-type algorithms based on the MWR data, evaluate the MWR-derived p-types and demonstrate the MWR as a robust instrument for p-type estimates. The parcel thickness method developed by Cantin and Bachand (1993) is applied to the MWR data. This method is particularly selected because of its dependency on 1000–850- and 850–700-hPa thickness layers as predictors for the p-type. Importantly, this method does not directly depend on the temperature profile as the MWR-retrieved temperature profile is found to have cold biases (Shrestha et al. 2022). While the temperature is a key factor that determines the thicknesses of the parcels, an explicit dependence on the quantitative thresholds for the temperature is avoided with this method as it is the function of the changes in temperature with height, not the absolute temperature. The MWR-retrieved p-types from six selected

NYSM profiler network sites are validated against the ground truth observations from the Meteorological Phenomena Identification Near the Ground (mPING) network (Elmore et al. 2014) and Automated Surface Observing System (ASOS) network (NOAA 1998) during a multiyear period from 2020 to 2022. The second goal of the study is to demonstrate the value of the MWR profiles to monitor and understand the thermodynamic processes taking place aloft in relation to the observed surface p-type, which is a much-needed information not available from the ASOS, mPING or Community Collaborative Rain, Hail and Snow Network (CoCoRaHS) that are all limited to the surface p-type reports only.

The paper is organized as follows: Details about the experimental site, methodology, and data are presented in section 2. The performance of the MWRs in estimating p-type is presented in section 3, with a wintry-mix case study in section 4. The real-time application in the NYSM operation is presented in section 5, followed by the conclusions of the study in section 6.

2. Experimental site, methodology, and data

The MWR provides thermodynamic profiles from the surface to 10 km with vertical resolution of 50 m up to 500 m, 100 m from 500 m to 2 km, and 250 m above 2 km and with temporal resolution of ~2 min. The data collected from six NYSM Profiler Network sites (Queens, Stony Brook, Red Hook, Albany, Jordan, and Buffalo; Fig. 1) from 2020 to 2022 (only November–April months considered) are used in this study. These six profiler network sites were strictly selected due to the availability of p-type observations from both mPING and ASOS in the vicinity. The six sites represent three distinct regions across New York; Queens and Stony Brook represent downstate New York City and the coastal region, Red Hook and Albany represent the mid-Hudson valley central region, and Jordan and Buffalo represent the upstate western region. Because off-zenith (20° elevation in north and south directions) retrievals are more accurate than zenith retrievals from the MWR during precipitation days (Xu et al. 2014), the profiles from the average of two off-zenith retrievals are used in this study and the data are further averaged over 10-min periods for the comparison purpose. Using the barometric formula, the MWR-retrieved height and temperature profiles are converted to pressure levels and a cubic spline interpolation is applied to obtain the data at 10-hPa resolution so that the data are available at mandatory pressure levels such as 1000, 850, and 700 hPa as defined by the American Meteorological Society (2014). Then, the parcel thickness method developed by Cantin and Bachand (1993) is applied to determine the parcel thickness layers using the MWR-retrieved profiles and diagnose p-type.

The parcel thickness method developed by Cantin and Bachand (1993) utilizes thickness of the 1000–700-hPa layer as the snow/rain line, which is further divided into two predictor layers as 1000–850 and 850–700 hPa to determine p-type. Since the mean temperature of the layer determines the thickness of that corresponding layer, the basic assumption of this method is that upper layer thickness of 850–700 hPa $>$ 1540 m and lower layer thickness of 1000–850 hPa $>$ 1310 m indicate a total thickness layer above 0°C and vice versa. For each upper layer thickness below and above 1540 m, the lower layer is further divided into: $<$1290 m, 1290–1310 m, and $>$1310 m to differentiate p-type [rain (RA), snow (SN), freezing rain (FZR), and sleet (SLT)]. For example, FZR is reported when thickness of 850–700 hPa $>$ 1540 m and 1000–850-hPa thickness of 1290–1310 m. The lower layer thickness $>$ 1310 m always yields RA. As this method was initially developed and used in southeastern Canada, the specific criteria threshold values as originally defined likely vary from those applicable in New York (Bourgouin 2000). Therefore, slightly different criteria values are developed based on our exploratory data analysis. Particularly, the lower layer thicknesses are increased by 10 m due to the observed mean bias error of 10 m between the radiosonde and MWR derived thicknesses (Shrestha et al. 2022). New criteria for upper layer thickness $>$ 1570 m are added to more precisely identify FZR and SLT. In addition, some near-surface temperature threshold criteria are also added to constrain certain p-type due to the accuracies of the MWR-retrieved temperature profiles being highest near the surface that degrades along the height (Shrestha et al. 2022). The detailed outline of the modified parcel thickness method is shown in Table 1.

The retrieved p-type results from the MWRs are compared against the ASOS observed p-type. The ASOS (https://www.weather.gov/asos/) is the primary surface weather observing network serving the nation's airports and weather service offices (NOAA 1998). They provide several surface meteorological parameters along with p-type. Each station has a precipitation detection sensor that differentiates between RA, SN, and FZR (but no sensor to detect SLT). Trained human observers manually augment ASOS reports to report SLT. Thus, SLT reporting is entirely dependent on ASOS staff; some underreporting and misdiagnosis can be expected due to the extra manual labor required. Similarly, the ASOS is also known to have some issues in reporting FZR and freezing drizzle automatically (Elmore et al. 2015; Landolt et al. 2019). In addition, the ASOS also has difficulty detecting p-type during mixed precipitation event or when precipitation is changing from one type to another, reporting as unknown precipitation "UP" (Landolt et al. 2019) and requiring manual augmentation. Therefore, it is found that augmented ASOS sites are more robust and reliable than nonaugmented sites that do not report SLT and mixed p-types (Reeves 2016). The MWR-retrieved p-type results from six NYSM Profiler sites (Queens, Stony Brook, Red Hook, Albany, Jordan, and Buffalo) are compared against p-type reports from six ASOS sites in the vicinity: LaGuardia Airport (LGA), ISLIP (ISP), Poughkeepsie (POU), Albany County Airport (ALB), Syracuse (SYR), and Buffalo International Airport (BUF) (see Fig. 1). Among these six selected ASOS sites in this study, only POU is a nonaugmented site. The average distances between the selected NYSM profiler and ASOS sites are presented in Table 2 and the ASOS data are available from Iowa State University Mesonet at https://mesonet.agron.iastate.edu/request/download.phtml?network=NY_ASOS.

Similarly, the MWR-retrieved p-type results are also compared against the mPING network (Elmore et al. 2014,

TABLE 1. A modified version of partial thickness method.

Thickness (m)		
850–700 hPa (H1)	1000–850 hPa (H2)	p-type
<1540	<1300	SN
	1300–1320	SLT/SN
	>1320	RA
≥1540	<1300	SN if H1 ≤ 1545
		SLT/SN if H1 > 1545
	1300–1320	FZR/RA
	>1320	RA
1570–1595	>1295	FZR/RA
1595–1605		FZR/SLT
≥1605	≥1310	FZR
	<1310	SLT
Additional conditions		
If retrieved p-type = SN and surface temperature ($T_{surface}$) > 0°C, change p-type to		RA/SN
If H2 > 1335 m and $T_{surface}$ > −1°C, p-type is		RA
If all temperature (T) ≤ −3°C throughout MWR profile (10 km), p-type is		SN
If $T_{surface}$ > 7°C, p-type is		RA
Within first near-surface 50 hPa, if all T > 0°C and T_{max} > 2°C, p-type is		RA
If retrieved[a] p-type = FZR or FZR/SLT and $T_{surface}$ < −3°C and H2 < 1320 m, change p-type to		SLT
If retrieved[b] p-type = SLT/SN or FZR/RA and $T_{surface}$ < −1°C, change p-type to		FZR/SN
If retrieved[b] p-type = RA and $T_{surface}$ < −1°C, change p-type to		FZR/RA
[b]If H1 > 1600 m and H2 > 1325 m		RA

[a] Only for those sites with surface pressure (Ps) ≈ 1000 hPa.
[b] Only for those sites with Ps ≫ 1000 hPa.

https://mping.ou.edu/). The mPING program archives p-type data that are reported by the public (referred to as "citizen scientists") from their locations using their cell phones or computers. Therefore, the mPING datasets contain high spatial and temporal observations of p-type from across the United States (Reeves 2016). However, the mPING reports have two significant shortcomings: 1) quality control is difficult as the reports are made by the general public, some of whom may not be trained to identify p-type correctly and may not follow consistent guidelines for reporting, and 2) reports are mostly limited to daytime observations in urban areas; overnight and rural area reports are less common. Nevertheless, the mPING reports are reasonably robust for comparison and validation purposes (Elmore et al. 2014). The mPING reports include 10 different p-types: snow and/or graupel, rain, drizzle, freezing drizzle, ice pellets/sleet, freezing rain, mixed rain and snow, mixed ice pellets and snow, mixed rain and ice pellets, and mixed freezing rain and ice pellets. The highest reported p-type category for each 10-min period within a 15-km radius of NYSM site is used for comparison with the MWR-retrieved p-type. The mPING observations within 15 km and 10 min are selected because the mPING reports of FZR and SLT agree with the ASOS at least 50% of the time with those criteria and that agreement decreases with increased distance and time from the ASOS observations (Elmore et al. 2014; Reeves 2016), which is basically due to high variability of FZR and SLT occurrence in space and time. Though the agreement increases with decrease in time and distance, the availability of mPING p-type reports is limited for the comparison.

Since mixed p-types are commonly reported by both the ASOS and mPING as well as those retrieved from the MWR, it is necessary to collapse the mixed p-type categories into one of the four major p-types (SN, RA, FZR, and SLT) for direct comparison. A match is considered when the MWR p-type agrees with or is in a mix with ASOS/mPING reports (example: FZR versus FZR/RA = FZR versus FZR). The mixed p-types are collapsed into one of the four major p-types with

TABLE 2. NYSM and ASOS site information.

NYSM site	Location (lat, lon)	ASOS site	Location (lat, lon)	Distance (km)
Queens	40.7343°, −73.8159°	LGA	40.7794°, −73.8803°	7
Stony Brook	40.9196°, −73.1333°	ISP	40.7939°, −73.1017°	14
Red Hook	41.9998°, −73.8841°	POU	41.6266°, −73.8842°	41
Albany	42.7516°, −73.8113°	ALB	42.7576°, −73.8036°	1
Jordan	43.0687°, −76.7699°	SYR	43.1112°, −76.1063°	54
Buffalo	42.9936°, −78.7946°	BUF	42.9408°, −78.7358°	8

TABLE 3. A 2 × 2 confusion matrix of the categorical forecast.

	Event observed	
Event forecast	Positive	Negative
Positive	True positive (TP)	False positive (FP)
Negative	False negative (FN)	True negative (TN)

the priority (greatest severity) order of FZR > SN > RA > SLT (example: FZR/SLT versus FZR/SN = FZR versus FZR; FZR/SLT versus RA/SN = FZR versus SN). Though SLT poses more threat than RA, it is given the lowest priority because of well-known issues of SLT reports from both mPING and ASOS (underreporting of SLT by the ASOS and overreporting of SLT by the mPING: Elmore et al. 2015; Reeves 2016). Finally, the performance of the MWR is reviewed using statistical measures based on a standard 2 × 2 contingency table (Table 3) in terms of probability of detection, precision, bias, and the Pierce skill score (Wilks 2006).

Based on Table 3, the following parameters are calculated for each p-type:

1) Probability of detection (POD) = TP/(TP + FN); perfect score of 1 ≠ perfect forecast
2) Precision = TP/(TP + FP); perfect score of 1 ≠ perfect forecast
3) Bias = (TP + FP)/(TP + FN); bias > 1 (overforecast), bias < 1 (underforecast), perfect score of 1 = perfect forecast
4) Pierce skill score (PSS) = POD − POFD, where probability of false detection (POFD) = FP/(FP + TN); perfect score of 1 = perfect forecast

3. Validation results and analysis

The accuracy of the MWR-retrieved p-types is validated and analyzed by comparing p-type reports from two different reference observations: mPING and ASOS in this section. Since the mPING observations are reported by the interested public while the ASOS observations are automated based on instrumental detection with manual augmentation on SLT reports by trained ASOS staffs, any observer and instrumental biases can lead to some discrepancies between two reference observations. Furthermore, the locations of the mPING observations vary in space and time while the observations from the ASOS are fixed, both reference observations may have additional discrepancies between them due to spatial and temporal variability. Therefore, both reference observations are compared against each other first to assess their agreements and potential biases in this section.

a. mPING versus ASOS observations

During the selected period of study (November–April of 2020–22), the frequency of p-types as reported by the mPING and ASOS for the three topographical regions of NYS are shown in Fig. 2. The highest reported mPING p-type category for each 10-min period within a 15-km radius of each ASOS site is used for comparison. As expected, both mPING and ASOS report RA and SN as the top two p-types across NYS. The frequency of RA observations in ASOS dataset is consistently higher than that of mPING while the frequency of SN observations in mPING dataset is comparable or higher than ASOS reports, consistent to observations across the continental United States as reported in Reeves (2016). Therefore, it appears that the mPING citizen scientists are less inclined to report RA than SN. Regarding the remaining p-types, the mPING reports are clearly more varied than the ASOS reports, except for FZR/SN, which is not reported by the mPING. The other p-types, apart from RA, SN, or its mix (RA/SN) comprise 10%–12% of mPING reports while just 2%–4% of ASOS reports. On average, the frequency of FZR or some combination that includes FZR in the mPING dataset (~3%) is somewhat comparable to that of ASOS (~2.6%); however, the frequency of SLT or some combination that includes SLT in the mPING reports (~9%) is considerably higher to that of ASOS reports (~0.7%). Such discrepancies in SLT reports between the mPING and ASOS could be either because 1) ASOS detection of SLT is not automated but rather augmented by the trained observer and hence, it could be possible at times when the SLT are underreported, or 2) the mPING users overreport SLT. Reeves (2016) reported that mPING users are often confused with wet SN or FZR and report them as SLT as the study showed that about 66% of mPING SLT reports were either SN or FZR. The highest reports of SN in upstate western region and RA in downstate region in both mPING and ASOS reports are consistent with the precipitation climatology of the NYS. Heavy lake-effect snow from the Great Lakes is very common in upstate western NYS while the warmer Atlantic Ocean temperature impacts the downstate region leading to more rain than snow.

The p-type comparison statistics from mPING and ASOS observations at the six selected sites: LGA, ISP, POU, ALB, SYR, and BUF are shown in Fig. 3. Considering the ASOS observations as "truth," the mPING reports of SN have POD ≥ 0.94 and RA has POD ≥ 0.80 for all the six sites (Fig. 3a). Similarly, SLT has POD ≥ 0.86 with the best value of 1 at LGA and SYR, i.e., no false negatives (misses). Though the POD for FZR has the best value of 1 at SYR, they are comparatively lower than other p-types at remaining sites (0.54 ≤ POD ≤ 0.83) and are negatively affected by higher misses. The precision values are much higher for RA and SN (≥0.91) followed by FZR (mostly ≥0.69) compared to SLT (0.19–0.53, Fig. 3b). In other words, mPING has the highest false alarm (false positive) rate for SLT among four p-types. As a result, very high bias values of 1.79–5.20 in the mPING SLT reports are observed (Fig. 3c), which is consistent with significantly higher observations of SLT from the mPING reports compared to the ASOS as seen in Fig. 2 and with previous studies by Reeves (2016).

A PSS value of 1 represents perfect forecast with no false alarms and misses. The mPING has PSS ≥ 0.80 for all three p-types: RA, SN, and SLT while FZR has PSS mostly ≤0.81 (Fig. 3d). Overall, the mPING p-types have PSS mostly above 0.7, suggesting reasonably reliable mPING reports. In summary, the mPING reports of FZR show the least agreement with the ASOS due to negative impact by high misses and

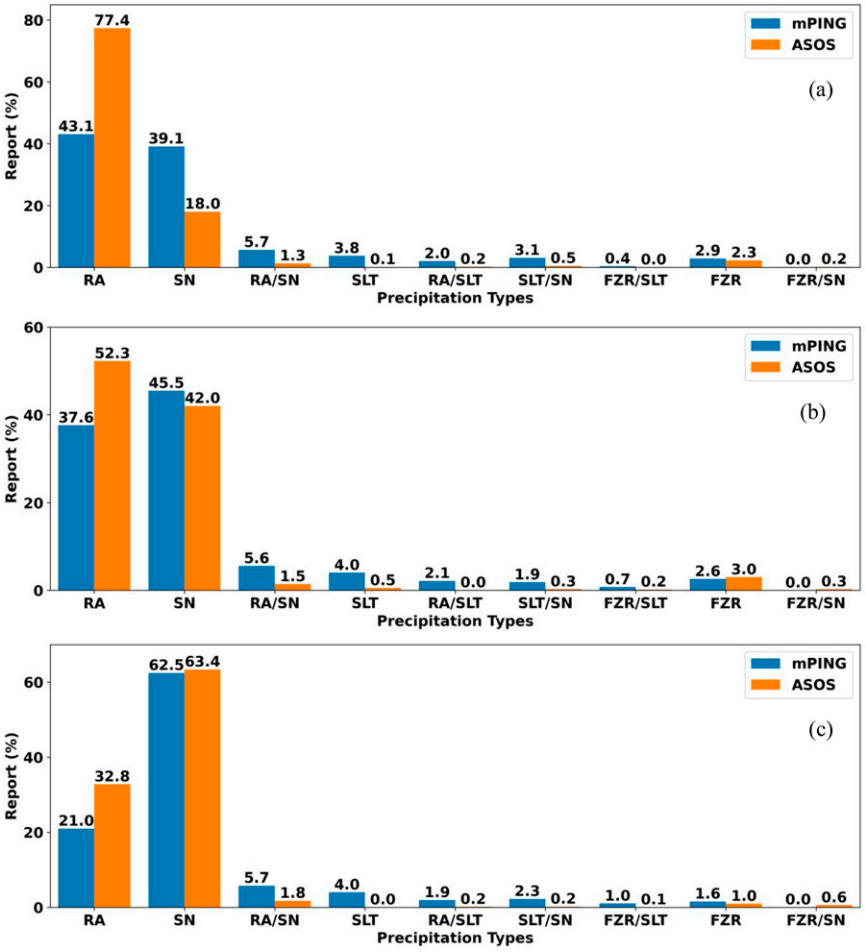

FIG. 2. The precipitation type reports from the mPING and ASOS at (a) downstate New York City region, (b) midstate Hudson Valley region, and (c) upstate western region during November–April of 2020–22.

because of the highest false alarms, the SLT reports are relatively better than the FZR.

b. *MWR retrievals versus mPING observations*

The MWR-retrieved p-types compared against the mPING observations at the six selected NYSM sites are shown in Fig. 4. The POD values are found to be the highest for RA (POD ≥ 0.95), followed by SN (POD ≥ 0.85), FZR (mostly ≥0.67), and SLT (mostly <0.50) across NYS (Fig. 4a). The precision values for SLT and SN are found to be the highest (≥0.92) while they are mostly greater than 0.75 for RA and the lowest for FZR (≤0.62, Fig. 4b). Such lower precision values for FZR are the result of higher false alarms and resulting overforecasts by the MWR (bias = 1.5–3.8, Fig. 4c). In contrast, the MWR underforecasts SLT (bias = 0.16–0.7) due to high misses as represented by low POD values. The overforecasting of FZR and underforecasting of SLT by the MWR could merely be due to 1) the underreporting of FZR and overreporting of SLT by mPING users as discussed in section 3a, and 2) p-type collapse scheme used with the priority order of FZR > SN > RA > SLT (MWR retrievals are biased toward FZR and away from SLT). Similar to the POD trend, the PSS values are the highest for RA (≥0.89), followed by SN (≥0.81), while they are mostly ≥0.58 for FZR and mostly ≤0.5 for SLT (Fig. 4d). In summary, the MWR provides high reliability in estimating RA, followed by SN, FZR and SLT. The MWR is found to have higher false alarms for FZR and higher misses for SLT, compared to the mPING reports.

c. *MWR retrievals versus ASOS observations*

The MWR retrieved p-types compared against the ASOS observations at the six selected NYSM sites are shown in Fig. 5. The POD values for SN and RA are reasonably high (POD ≥ 0.95) while for FZR, the POD values tend to decrease from 0.88 at Queens (QUEE) to 0.46 at Buffalo (BUFF) (Fig. 5a). Coincidentally, this decreasing trend observed from QUEE to BUFF matches with their increasing trend in elevations (QUEE to BUFF, site elevations increase from 53 to 186 m). The POD values for SLT are very different from one site to another. The precision values are the highest

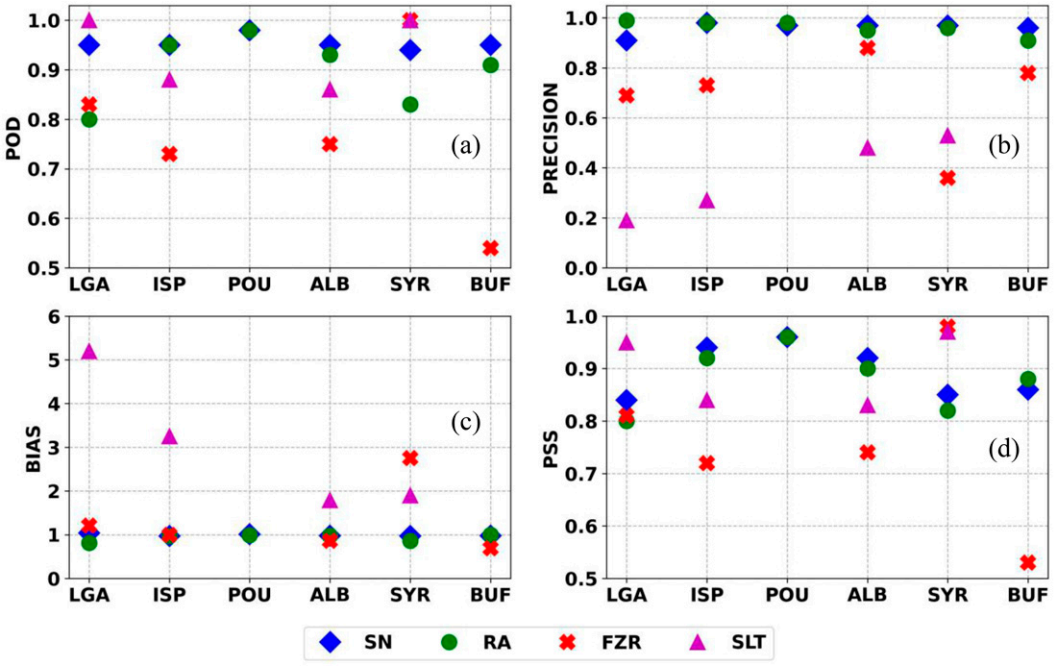

FIG. 3. Comparison of p-type results between mPING (forecasts) and ASOS (observations) in terms of (a) POD, (b) precision, (c) bias, and (d) PSS.

for RA (≥0.99), followed by SN (≥0.89), SLT (mostly ≥0.83) and FZR (0.33–0.73). Similar to the comparison results with mPING FZR reports (Fig. 4c), the MWR also overforecasts FZR compared to the ASOS reports; however, the biases are much lower, ≤1.58 (Fig. 5c). The MWR severely underforecasts SLT at Stony Brook (STON), Jordan (JORD), and BUFF. The PSS values are nearly identical to the POD values for all four p-types due to low POFD (Fig. 5d). In summary,

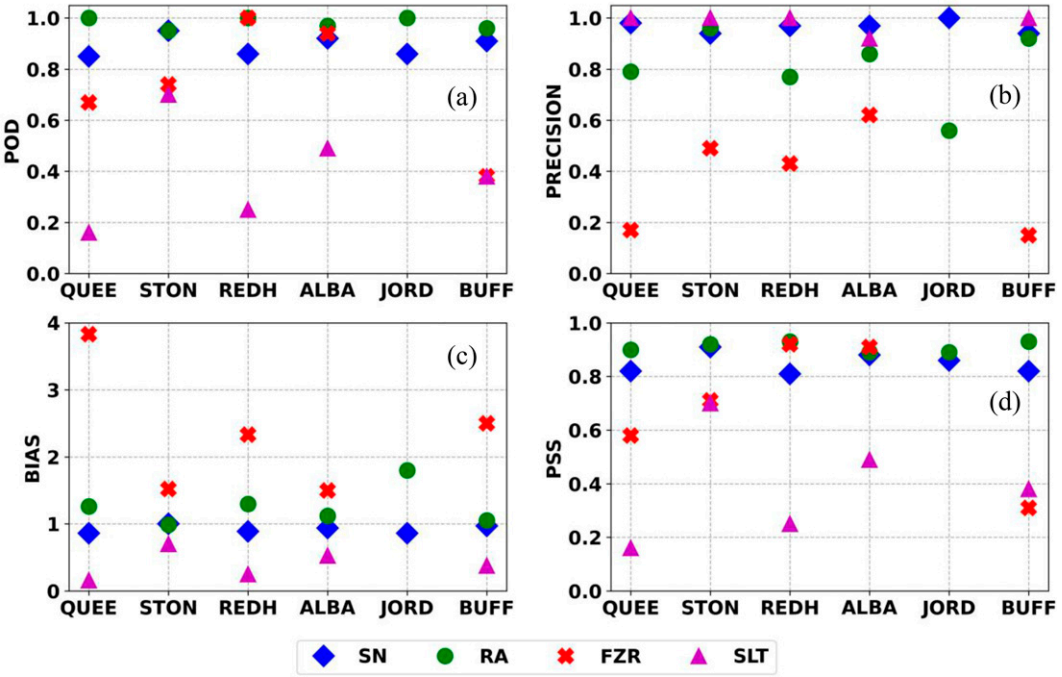

FIG. 4. Comparison of p-type results between MWR retrievals and mPING reports in terms of (a) POD, (b) precision, (c) bias, and (d) PSS.

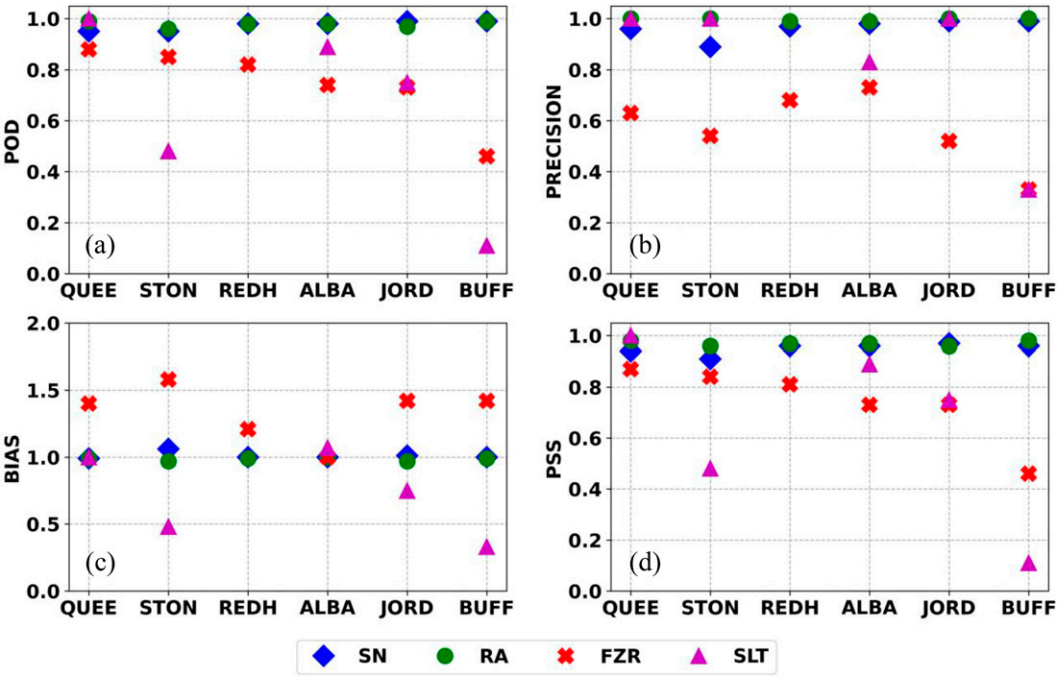

FIG. 5. Comparison of p-type results between MWR retrievals and ASOS observations in terms of (a) POD, (b) precision, (c) bias, and (d) PSS.

the MWR provides high reliability in RA, followed by SN, FZR and SLT, and the MWR is found to have higher false alarms for FZR and higher misses for SLT compared to ASOS reports, a similar trend to that observed for MWR-mPING comparison (Fig. 4); however, the MWR-retrieved p-types are in better agreement with ASOS than mPING reports.

4. Case study of wintry mix event

This section presents a case study on the temporal evolution of p-types during a major winter storm at Albany on 3–4 February 2022 (https://www.weather.gov/btv/Long-Duration-Snowstorm-and-Mixed-Precipitation-Event-on-3-4-February-2022). This event was particularly selected because the winter storm brought a variety of wintry mix of all four major p-types: RA, SN, FZR, and SLT. A plume of highly anomalous moisture persisted over the Northeast region of the United States for about 48 h and the favorable upper-level jet dynamics with associated upper-level divergence resulted in a prolonged period of heavy precipitation during the event. The main highlight of the event was 12+ hours of SLT totaling around 2 in. at Albany, a region in the mid-Hudson Valley. However, it was mostly SN across western upstate New York and RA across downstate and around New York City. This case study is presented to demonstrate the effectiveness of the MWR in real-time monitoring of p-types and capturing the transition of p-type from one to another. The 40 h of p-type observations from the MWR retrievals at the Albany, nearby ASOS site (ALB) and mPING (reports from within 15-km radius of the Albany profiler site) are shown in Fig. 6a. The p-type data are shown every 10 min when available from each observation along with the MWR-derived skew T–log$p$ plots for four different times in Figs. 6b–e.

The MWR-retrieved p-types are in agreement with the mPING and ASOS reports during the event. It was all RA on 3 February with a shift to FZR toward the end of the day at 2300 UTC. The FZR event lasted about 4 h and transitioned into SLT starting 0200–0300 UTC until mid-4 February. After that, SN was observed for the rest of the day. The MWR effectively captures such transition of p-type for 40 h, consistent with both ASOS and mPING observations. The MWR-retrieved temperature profile shows the temperature above freezing (>0°C) in a sufficiently deep layer below 750 mb (1 mb = 1 hPa), leading to RA at 1200 UTC 3 February (Fig. 6b). But because an upper inversion layer (900–750 mb) existed and near surface temperature decreased later in the day, this gave rise to an upper layer warm nose (900–700 mb) and shallow lower subfreezing layer below 900 mb with surface temperature of −2.5°C, causing supercooled liquid drops from the upper layer to freeze on surface contact, resulting in FZR at 0000 UTC 4 February (Fig. 6c). By 1100 UTC, as the surface temperature decreased further to −8°C, this resulted in a deep subfreezing layer below 850 mb and the supercooled liquid drops from the upper-layer warm nose to freeze into SLT (Fig. 6d). Later by 1800 UTC, the total vertical profile of temperature was below freezing that gave rise to the SN at the surface (Fig. 6e). This case study of wintry mix event further validates the MWR-retrieved p-types with comparable accuracy to the mPING and ASOS reports and demonstrates its capability in monitoring high temporal p-type transition. In addition, the MWR thermodynamic profiles (skew T–log$p$ plots) allow forecasters to

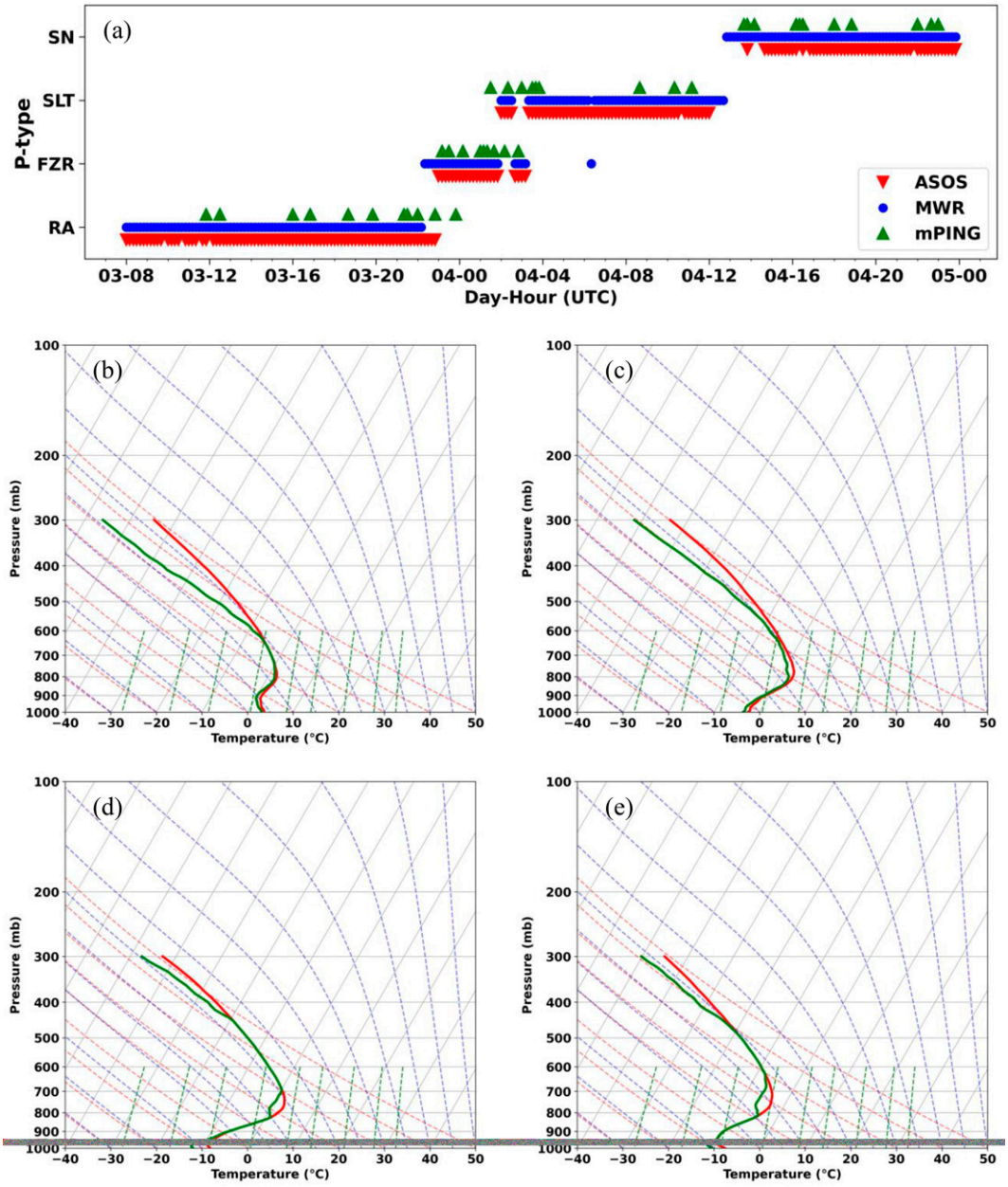

FIG. 6. (a) The MWR-retrieved p-types along with ASOS and mPING p-type reports during 3–4 Feb 2022 at Albany, and skew T–log$p$ plots at (b) 1200 UTC 3 Feb, and at (c) 0000, (d) 1100, and (e) 1800 UTC 4 Feb.

monitor the evolution and vertical extent of any upper layer warm nose and near surface subfreezing layer associated with FZR and SLT and issue timely warnings of any possible ice storm.

5. Real-time application

The NYSM profiler network data are collected, archived, and disseminated in real time every 10 min. A time–height cross section plots of wind, aerosol backscatter, temperature, liquid density, vapor density and relative humidity are displayed in real-time and are publicly available at the NYSM profiler web page: http://www.nysmesonet.org/networks/profiler, from all 17 profiler sites. In addition, the derived products such as MWR-retrieved p-types based on section 2 and associated skew T–log$p$ plots are also displayed at the NYSM profiler web page and the screenshot of one example is shown in Fig. 7 along with time–height cross-section plots for MWR-retrieved temperature and relative humidity. All data are updated every 10 min and can be viewed for the last 24 h from the time of viewing. These real-time data are used in NWS operations and as in the

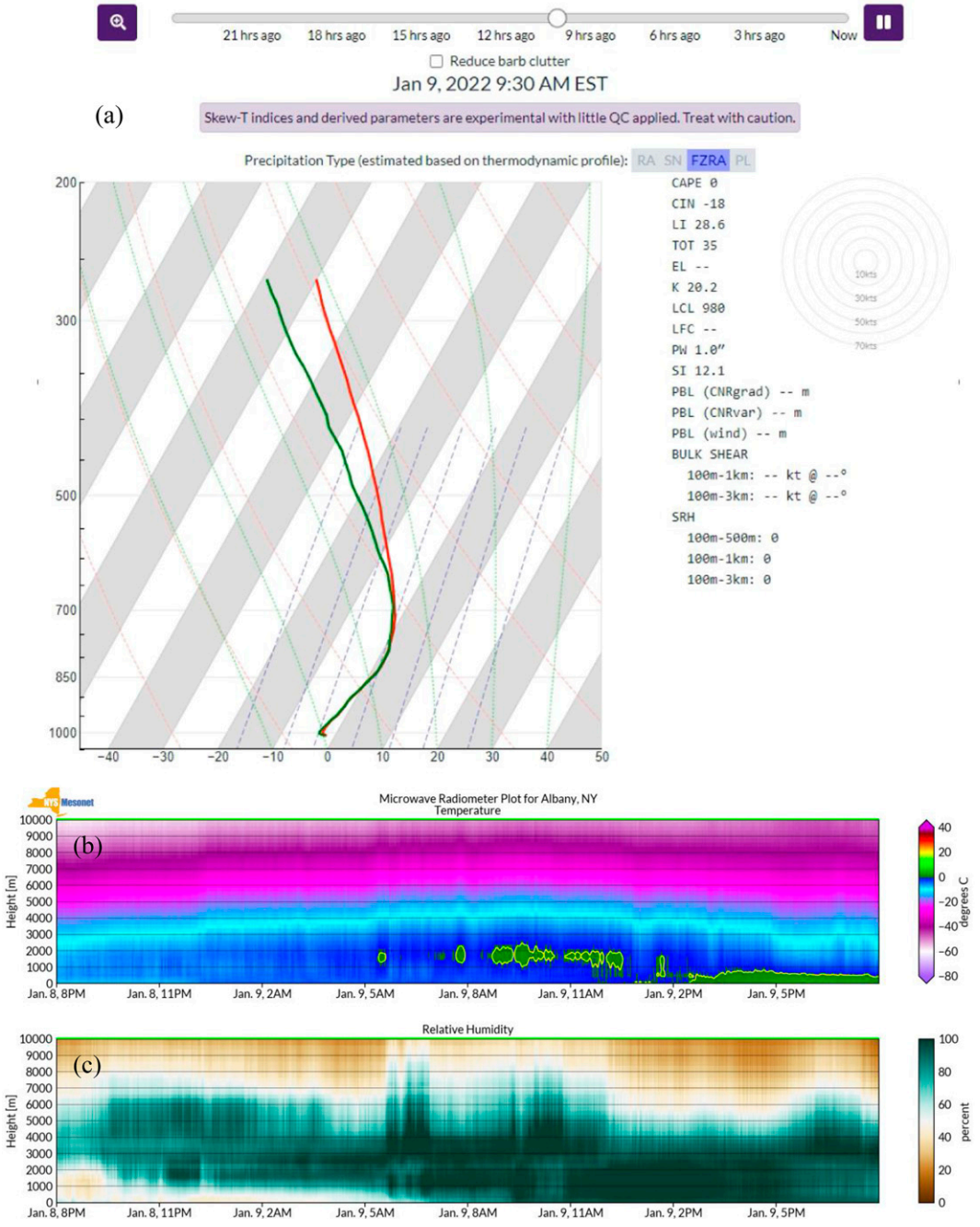

FIG. 7. Real-time display of MWR-retrieved (a) p-type and its associated skew T–log$p$ plot, (b) temperature (°C), and (c) relative humidity (%) at Albany for 24 h starting at 2000 LT 8 Jan 2022.

example shown in Fig. 7, the data were used by the NWS Albany WFO to monitor the wintry mix event on 9–11 January 2022. Therefore, having the continuous thermodynamic and kinematic profiles, and p-type estimates with its associated skew T–log$p$ plots every 10 min (a significant advantage over twice daily NWS radiosonde updates) helps forecasters to monitor the evolution of winter storm in real time and provides confidence in issuing timely warnings and alerts.

6. Conclusions

Many operational techniques based on radiosonde profiles have been developed to determine p-types. However, low temporal sampling and spatial coverage of the NWS radiosonde network data limit our ability to determine p-type in real-time and to monitor fine-scale microphysical and thermodynamic processes that govern p-type. Because continuous thermodynamic profiles are available from the MWR every

2 min, this paper presents an application and evaluation of the MWRs from the NYSM profiler network to accurately retrieve p-type. A modified version of the parcel thickness method is applied to the MWR data to diagnose p-type, and those results are compared against the reports from the mPING and ASOS at six selected NYSM profiler network sites (Queens, Stony Brook, Red Hook, Albany, Jordan, and Buffalo) during November–April of 2020–22. The mPING and ASOS data are compared against each other to assess any discrepancies between them due to observer, instrument, spatial and temporal variability before comparing them with the MWR retrievals. Compared to the ASOS reports, the mPING observers are found to be less inclined to report RA than SN while they are more inclined to report SLT than FZR. The mixed p-type reports are normally higher in mPING than ASOS observations. The mPING SLT has the lowest precision and relatively high bias values while the mPING FZR has the lowest POD and PSS values. Overall, the mPING ptypes have PSS mostly > 0.7 across the selected six sites, demonstrating its reasonable accuracy compared to the ASOS reports.

When compared against the mPING reports, the MWR has the best PSS for RA (PSS ≥ 0.89) followed by SN (PSS ≥ 0.81), FZR (mostly PSS ≥ 0.58) and SLT (mostly PSS ≤ 0.49). Similarly, when compared against the ASOS reports, the MWR also has the best PSS for RA (PSS ≥ 0.96), followed by SN (PSS ≥ 0.91), FZR (mostly PSS ≥ 0.73) and SLT (mostly PSS ≥ 048), which are comparatively better than compared to mPING. Relative to both mPING and ASOS reports, the MWR overforecasts FZR and underforecasts SLT which could be due to underreporting of FZR and overreporting of SLT in the mPING observations, underreporting of SLT and known issues with FZR in the ASOS observations and the p-type collapse scheme used that is biased toward FZR and away from SLT. Though some known discrepancies in FZR and SLT reports from both the mPING and ASOS datasets may have impacted the MWR comparison results, those results can be further improved with the refinement of the parcel thickness method or the application of robust and explicit temperature dependent area method that have better performance than other available techniques (Bourgouin 2000), a part of future work. Overall, the MWR provides high accuracy in estimating RA and SN and a reasonable accuracy in estimating FZR and SLT that is still considerably better than the results from the numerical models such as the RAP, NAM, and GFS (Elmore et al. 2015).

The continuous thermodynamic profiles from the MWR (and wind profiles from the Doppler lidar) and p-type estimates with its associated skew T–log$p$ plot every 10 min (http://www.nysmesonet.org/networks/profiler) from all 17 Profiler sites provide significant advantage over twice daily NWS radiosondes in monitoring the evolution of winter storm in real-time and better understanding the favorable conditions associated with certain p-types, especially FZR and SLT that pose hazardous winter weather condition. Such information allows the weather forecasters to issue timely and accurate warnings and alerts. In addition, p-types estimated from the NYSM surface network (Wang et al. 2021, http://www.nysmesonet.org/weather/winter) are also available to provide better spatial coverage across the NYS (126 sites, spaced an average of 30 km apart). Overall, the NYSM supports real-time monitoring of high-impact winter weather in a regional scale; provides the high spatial and temporal resolution data necessary to initialize and validate numerical models; and potentially aid in numerical model development and forecasting.

Acknowledgments. This work is partially supported by the Observations Program within the NOAA/OAR Weather Program Office under Award NA21OAR4590376. Additional funding is provided by the NOAA/National Weather Service Program Office (NWSPO) under Award NA22NWS4690023. The original funding for the NYSM was provided by FEMA Grant FEMA-4085-DR-NY, with the continued support of the National Mesonet Program; NYS Division of Homeland Security and Emergency Services; the state of New York; the Research Foundation for the State University of New York (SUNY); the University at Albany, SUNY; the Atmospheric Sciences Research Center (ASRC) at SUNY Albany; and the Department of Atmospheric and Environmental Sciences (DAES) at SUNY Albany. The authors greatly appreciate the precipitation-type data from the ASOS and mPING networks. The authors declare that they have no real or perceived financial conflicts of interest.

Data availability statement. The NYSM Profiler Network data are available at http://www.nysmesonet.org/weather/requestdata according to the NYSM data policy stated in the webpage. The ASOS data are available at https://mesonet.agron.iastate.edu/request/download.phtml?network=NY_ASOS and the mPING data are available through API at https://mping.ou.edu/static/mping/access.html.

REFERENCES

Ahrens, C. D., and R. Henson, 2018: *Meteorology Today: An Introduction to Weather, Climate, and the Environment.* Cengage Learning, 656 pp.

American Meteorological Society, 2014: Mandatory levels. Glossary of Meteorology, https://glossary.ametsoc.org/wiki/Mandatory_level.

Baldwin, M., R. Treadon, and S. Contorno, 1994: Precipitation type prediction using a decision tree approach with NMCs mesoscale eta model. Preprints, *10th Conf. on Numerical Weather Prediction*, Portland, OR, Amer. Meteor. Soc., 30–31.

Bhaskaran, K., S. Hajat, A. Haines, E. Herrett, P. Wilkinson, and L. Smeeth, 2009: Effects of ambient temperature on the incidence of myocardial infarction. *Heart*, **95**, 1760–1769, https://doi.org/10.1136/hrt.2009.175000.

Bourgouin, P., 2000: A method to determine precipitation types. *Wea. Forecasting*, **15**, 583–592, https://doi.org/10.1175/1520-0434(2000)015<0583:AMTDPT>2.0.CO;2.

Cantin, A., and D. Bachand, 1993: Synoptic pattern recognition and partial thickness techniques as a tool for precipitation types forecasting associated with a winter storm. Centre Meteorologique du Quebec Tech. Note 93N-002, 9 pp.

Cimini, D., M. Nelson, J. Guldner, and R. Ware, 2015: Forecast indices from a ground-based microwave radiometer for

operational meteorology. *Atmos. Meas. Tech.*, **8**, 315–333, https://doi.org/10.5194/amt-8-315-2015.

Dahlquist, M., and Coauthors, 2016: Short-term departures from an optimum ambient temperature are associated with increased risk of out-of-hospital cardiac arrest. *Int. J. Hyg. Environ. Health*, **219**, 389–397, https://doi.org/10.1016/j.ijheh.2016.03.005.

Derouin, R., 1973: Experimental forecast of freezing level(s), conditional precipitation type, surface temperature, and 50-meter wind, produced by the planetary boundary layer (PBL) model. NOAA Tech. Procedures Bull. 101, 8 pp., https://www.weather.gov/media/mdl/TPB_101.pdf.

Elmore, K. L., Z. L. Flamig, V. Lakshmanan, B. T. Kaney, V. Farmer, H. D. Reeves, and L. S. Rothfusz, 2014: mPING: Crowd-sourcing weather reports for research. *Bull. Amer. Meteor. Soc.*, **95**, 1335–1342, https://doi.org/10.1175/BAMS-D-13-00014.1.

——, H. M. Grams, D. Apps, and H. D. Reeves, 2015: Verifying forecast precipitation type with mPING. *Wea. Forecasting*, **30**, 656–667, https://doi.org/10.1175/WAF-D-14-00068.1.

Illingworth, A. J., and Coauthors, 2019: How can existing ground-based profiling instruments improve European weather forecasts? *Bull. Amer. Meteor. Soc.*, **100**, 605–619, https://doi.org/10.1175/BAMS-D-17-0231.1.

Landolt, S. D., J. S. Lave, D. Jacobson, A. Gaydos, S. DiVito, and D. Porter, 2019: The impacts of automation on present weather-type observing capabilities across the conterminous United States. *J. Appl. Meteor. Climatol.*, **58**, 2699–2715, https://doi.org/10.1175/JAMC-D-19-0170.1.

Löhnert, U., and O. Maier, 2012: Operational profiling of temperature using ground-based microwave radiometry at Payerne: Prospects and challenges. *Atmos. Meas. Tech.*, **5**, 1121–1134, https://doi.org/10.5194/amt-5-1121-2012.

NOAA, 1998: Automated Surface Observing System: ASOS user's guide. NOAA, 74 pp.

NOAA/National Centers for Environmental Information, 2022: U.S. Billion-dollar Weather and Climate Disasters, 1980–present (NCEI Accession 0209268). NOAA, accessed 31 October 2022, https://doi.org/10.25921/stkw-7w73.

Ralph, F. M., and Coauthors, 2005: Improving short-term (0–48 h) cool-season quantitative precipitation forecasting: Recommendations from a USWRP workshop. *Bull. Amer. Meteor. Soc.*, **86**, 1615–1632, https://doi.org/10.1175/BAMS-86-11-1615.

Ramer, J., 1993: An empirical technique for diagnosing precipitation type from model output. Preprints, *Fifth Int. Conf. on Aviation Weather Systems*, Vienna, VA, Amer. Meteor. Soc., 227–230.

Reeves, H. D., 2016: The uncertainty of precipitation-type observations and its effect on the validation of forecast precipitation type. *Wea. Forecasting*, **31**, 1961–1971, https://doi.org/10.1175/WAF-D-16-0068.1.

——, K. L. Elmore, A. Ryzhkov, T. Schuur, and J. Krause, 2014: Sources of uncertainty in precipitation type forecasting. *Wea. Forecasting*, **29**, 936–953, https://doi.org/10.1175/WAF-D-14-00007.1.

Ryti, N. R. I., and Coauthors, 2017: Cold spells and ischaemic sudden cardiac death: Effect modification by prior diagnosis of ischaemic heart disease and cardioprotective medication. *Sci. Rep.*, **7**, 41060, https://doi.org/10.1038/srep41060.

Schuur, T. J., H.-S. Park, A. V. Ryzhkov, and H. D. Reeves, 2012: Classification of precipitation types during transitional winter weather using the RUC model and polarimetric radar retrievals. *J. Appl. Meteor. Climatol.*, **51**, 763–779, https://doi.org/10.1175/JAMC-D-11-091.1.

Shrestha, B., J. A. Brotzge, J. Wang, N. Bain, C. D. Thorncroft, E. Joseph, J. Freedman, and S. Perez, 2021: Overview and application of the New York State Mesonet Profiler Network. *J. Appl. Meteor. Climatol.*, **60**, 1591–1611, https://doi.org/10.1175/JAMC-D-21-0104.1.

——, ——, and ——, 2022: Evaluation of the New York State Mesonet Profiler Network Data. *Atmos. Meas. Tech.*, **15**, 6011–6033, https://doi.org/10.5194/amt-15-6011-2022.

USDOT Federal Highway Administration, 2014: Winter Weather Highway Safety. USDOT Federal Highway Administration, 2 pp., https://www.highways.org/wp-content/uploads/2014/02/Brochure-FINAL-LoRes.pdf.

Wang, J., J. Brotzge, J. Shultis, and N. Bain, 2021: Enhancing icing detection and characterization using the New York State Mesonet. *J. Atmos. Oceanic Technol.*, **38**, 1499–1514, https://doi.org/10.1175/JTECH-D-20-0215.1.

Ware, R., R. Carpenter, J. Güldner, J. Liljegren, T. Nehrkorn, F. Solheim, and F. Vandenberghe, 2003: A multichannel radiometric profiler of temperature, humidity, and cloud liquid. *Radio Sci.*, **38**, 8079, https://doi.org/10.1029/2002RS002856.

Wilks, D. S., 2006: *Statistical Methods in the Atmospheric Sciences*. 2nd ed. International Geophysics Series, Vol. 100, Academic Press, 648 pp.

Xu, G., R. Ware, W. Zhang, G. Feng, K. Liao, and Y. Liu, 2014: Effect of off-zenith observations on reducing the impact of precipitation on ground-based microwave radiometer measurement accuracy. *Atmos. Res.*, **140–141**, 85–94, https://doi.org/10.1016/j.atmosres.2014.01.021.

——, B. Xi, W. Zhang, C. Cui, X. Dong, Y. Liu, and G. Yan, 2015: Comparison of atmospheric profiles between microwave radiometer retrievals and radiosonde soundings. *J. Geophys. Res. Atmos.*, **120**, 10 313–10 323, https://doi.org/10.1002/2015JD023438.